

Supplementary Information

High resolution analytical electron microscopy reveals cell culture media induced changes to the chemistry of silver nanowires

Shu Chen,¹ Ioannis G. Theodorou,¹ Angela E. Goode,¹ Andrew Gow,² Stephan Schwander,³
Junfeng (Jim) Zhang,⁴ Kian Fan Chung,⁵ Teresa D. Tetley,⁵ Milo S. Shaffer,⁶ Mary P. Ryan¹
* and Alexandra E. Porter.^{1*}

¹Department of Materials and London Centre for Nanotechnology, Imperial College London,
Exhibition Road, London SW7 2AZ, UK

²Department of Pharmacology and Toxicology at Rutgers University, Piscataway, NJ, USA

³Department of Environmental and Occupational Health, University of Medicine and Dentistry
(UMDNJ) School of Public Health, New Jersey, USA

⁴Department of Preventive Medicine, Keck School of Medicine, University of Southern
California, USA

⁵National Heart and Lung Institute, Imperial College London, UK

⁶Department of Chemistry and London Centre for Nanotechnology, Imperial College London,
Exhibition Road, London SW7 2AZ, UK

This SI file includes 20 pages, 2 tables and 15 figures.

Experimental

Synthesis of AgNWs

The AgNWs were synthesised using a modification of the polyol process, originally developed by Xia *et al.*,¹ In a typical synthesis, 3.5 mL ethylene glycol (EG; Sigma-Aldrich, anhydrous, 99.8%) solution of 65 mM of Silver nitrate (AgNO₃, Sigma-Aldrich, >99%,) and poly(vinyl pyrrolidone) (PVP, Sigma-Aldrich, average molecular weight Mw≈360k, [vinyl pyrrolidone]/[Ag]=1.5) were added drop-wise into 5.5 mL EG solution refluxed at 160 °C. The reaction mixture was further refluxed at 160 °C for 90 min. After diluting the reaction mixture five times by volume with acetone, the AgNWs were collected by centrifugation at 4500 rpm (2558 g) for 10 min. The AgNWs were further purified by repeating the washing process in ethanol and then deionized water three times respectively.

Scanning electron microscopy

The morphology and size distribution of as-synthesized AgNWs were characterized using a LEO1525 Field Emission Gun Scanning Electron Microscope (FEG-SEM, Carl Zeiss Microscopy GmbH, UK). The SEM was operated in secondary electron mode with an accelerating voltage of 5 kV. The AgNW dimensions were measured using ImageJ freeware.²

Transmission electron microscopy sample preparation

AgNWs were incubated in a temperature-controlled incubator set at 37 °C for 0.25, 1, 6 and 24 h respectively, at a concentration of 5 µg/mL (on a Ag atom basis as determined by ICP-OES), in the dark. The media used for incubation were Dulbecco's Modified Eagle's Medium (DMEM, without L-glutamine, Sigma), Roswell Park Memorial Institute medium (RPMI-1640, without L-glutamine, Sigma), DCCM-1 (without L-glutamine, Biological Industries, Israel), inorganic salts and proteins extracted from DCCM-1, phosphate buffered saline (PBS, 1 X concentration, pH 7.4, (without) CaCl₂, (without) MgCl₂, Gibco, Life Technologies), 5 mass % cysteine/PBS (L-cysteine HCl monohydrate, Sigma), and 5 % BSA/PBS (albumin, from bovine serum, lyophilized powder, ≥96%, Sigma). DCCM-1 was separated to its inorganic salt and protein constituents using ultra-centrifugal filter units (Amicon[®] Ultra, Millipore) with a pore size of 3 kDa (molecule mass), which is small enough to capture all proteins in DCCM-1.³

The filtrates, containing only inorganic salts, were collected and used immediately for incubation. The proteins collected at the filter membrane were thoroughly washed with PBS six times and dispersed in PBS for incubation.

After incubation, AgNWs were collected by centrifugation (16000 g, 20 min), washed with DI-H₂O three times and dispersed in DI-H₂O. Then the AgNWs were drop cast on to 300 mesh holey carbon film TEM grids and immediately placed under vacuum and in the dark for drying and storage, to avoid exposure to contamination or reactions induced by ambient atmosphere. Each experiment was repeated three times and more than 100 AgNWs from each sample were imaged and analyzed by TEM.

Transmission electron microscopy

High resolution transmission electron microscopy (HRTEM) and high angle annular dark field scanning transmission electron microscopy (HAADF-STEM), combined with (Energy-dispersive X-ray spectroscopy) EDX analysis were carried out using an FEI Titan 80/300 fitted with a C_s (image) corrector, monochromator and EDX detector (EDAX, Leicester UK). The intensity of a HAADF-STEM image is proportional to Z^n ($n \sim 2$), therefore this technique is highly sensitive to atomic number (Z) variations within the sample. An accelerating voltage of 300 kV was used for both TEM and STEM experiments. For STEM experiments, a convergence semi-angle of 14 mrad was used, with an inner and outer HAADF collection angle of 49 and 239 mrad, respectively. The probe diameter was <0.5 nm. Selected area electron diffraction (SAED) was performed using a camera length of 600 mm and an aperture size of 130-550 nm. The SAED patterns were analyzed using DiffTools (version 3.7), an electron diffraction software package for DigitalMicrograph™ (Mitchell DRG, 2008).

ICP-OES and pH analysis

AgNWs were incubated in cell culture media at 37°C at a concentration of 5 µg/mL for 1, 6, 24, 72, 124 and 168 h ($n = 3$). Aliquots were collected at each time point and filtered through 2 kDa centrifuge membranes (Sartorius Stedim VIVACON 500). The amount of solubilized silver in the filtrates was analyzed using Inductively Coupled Plasma–Optical Emission Spectroscopy with a silver detection limit of 0.6 ppb (ICP-OES, Thermo Scientific, UK). In a control experiment, 17.0 µg/mL of AgNO₃ (equal to

Ag concentration of 10 $\mu\text{g/mL}$) DI- H_2O and DCCM-1 solutions were incubated at 37°C for 0.5 h. After incubation, aliquots were extracted and filtered through 2 kDa centrifuge membranes for ICP-OES analysis ($n = 3$).

For sulfur content analysis, AgNWs were incubated in PRMI-1640, DMEM and DCCM-1 filtrate at 37°C at concentrations of 5 and 50 $\mu\text{g/mL}$ respectively for 1, 6 and 24 h ($n = 3$). Aliquots were collected at each time point and filtered through 2 kDa centrifuge membranes for ICP-OES analysis of sulfur element. The pH measurements of PRMI-1640, DMEM and DCCM-1 at 37°C incubated with AgNWs at concentrations of 5 and 50 $\mu\text{g/mL}$ respectively for 1, 6 and 24 h ($n = 3$) were carried out by a pH meter (VWR International SympHony SB70P Benchtop Digital pH Meter, UK) at room temperature.

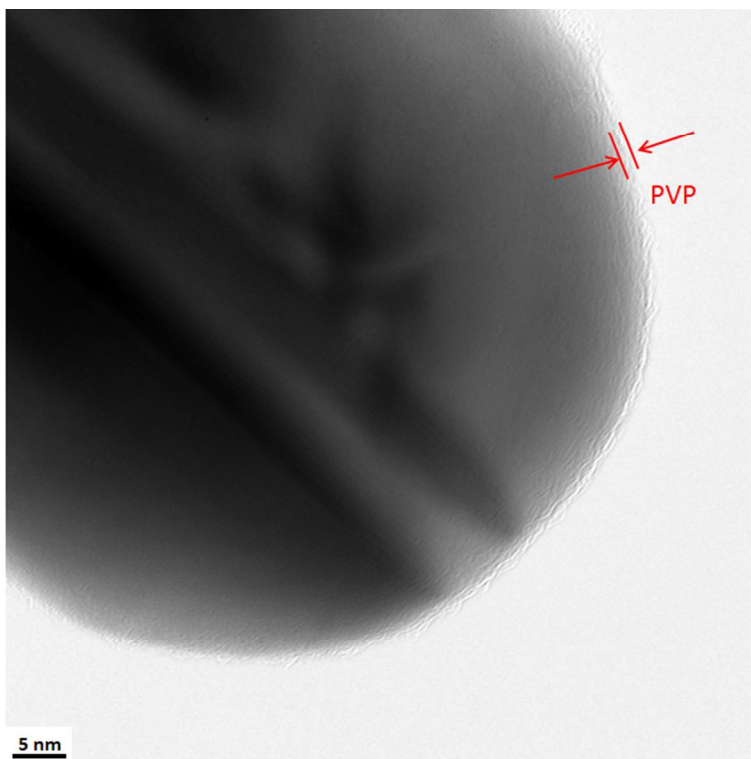


Figure 1S. A HRTEM image shows the PVP layer on a AgNW surface.

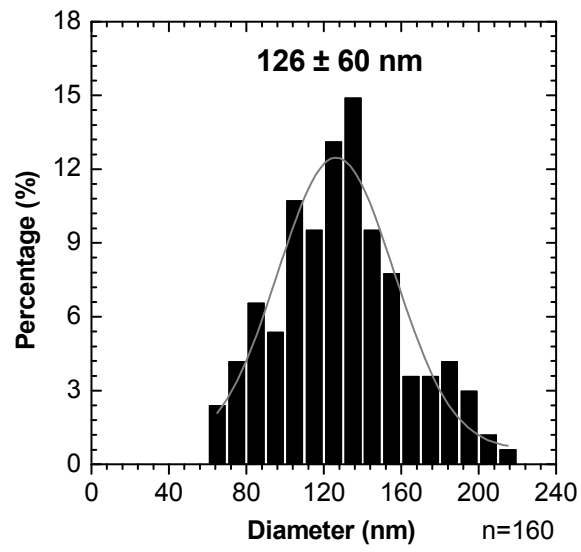


Figure 2S. The AgNPs diameter distribution in the as-synthesized AgNWs samples.

Table 1S. Crystal structure information of various silver compounds based on the Inorganic Crystal Structure Database. Only the principal peak intensities ($\geq 20\%$) are listed.⁴

h	k	l	d (Å)	2Theta (deg)	Intensity (%)
Ag : Cubic, ICSD ref (01-087-0597)					
1	1	1	2.35917	38.115	100
2	0	0	2.0431	44.299	45.7
2	2	0	1.44469	64.443	22.5
3	1	1	1.23204	77.397	22.2
Ag₂O : Cubic, ICSD ref (01-041-1104)					
1	1	1	2.7290	32.791	100
2	0	0	2.3620	38.067	28
AgCl : Cubic, ICSD ref (01-031-1238)					
1	1	1	3.20300	27.831	50
2	0	0	2.77400	32.244	100
2	2	0	1.96200	46.234	50
Ag₃PO₄ : Cubic, ICSD ref (00-006-0505)					
2	1	0	2.68900	33.293	100
2	1	1	2.45400	36.588	35
3	2	0	1.66760	55.022	20
Ag₂S: Monoclinic, ICSD ref(00-014-0072)					
-1	1	1	3.437	25.902	35
0	1	2	3.383	26.323	20
1	1	1	3.08	28.967	60
-1	1	2	2.836	31.521	70
1	2	0	2.664	33.614	45
-1	2	1	2.606	34.385	100
0	2	2	2.583	34.701	70
1	1	2	2.456	36.557	70
1	2	1	2.44	36.806	80
0	1	3	2.421	37.105	60
-1	0	3	2.383	37.719	75
0	3	1	2.213	40.74	45
2	0	0	2.083	43.407	45
-1	2	3	1.963	46.209	20

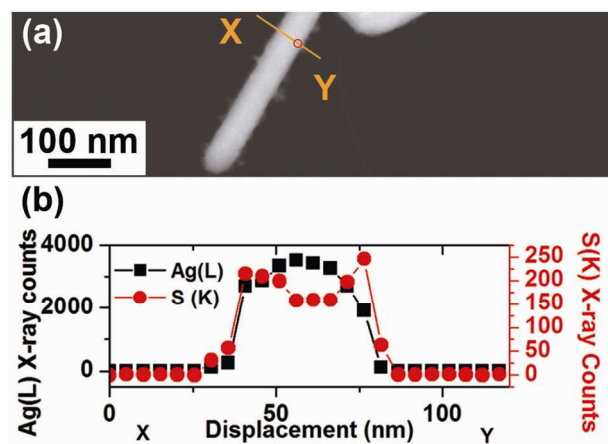


Figure 3S. (a) A HAADF-STEM image of the AgNW shown in Fig. 2c. A STEM-EDX line profile was collected along the line XY. (b) The formation of a layer of sulfidized silver on the surface of the AgNWs was confirmed by EDX. The X-ray counts within an energy window around the Ag (L) and S (K) peaks were extracted along the line X-Y.

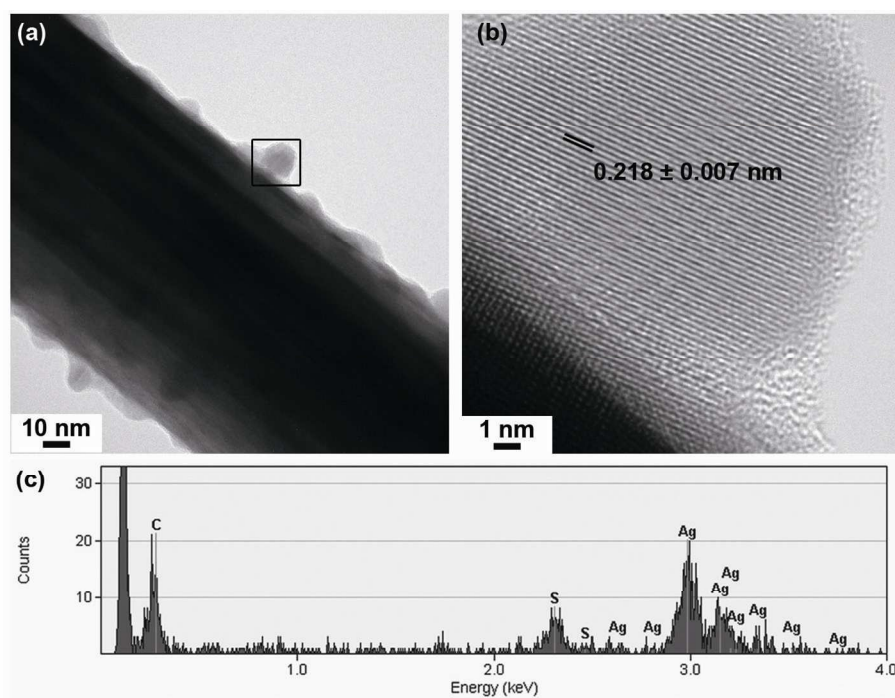


Figure 4S: TEM characterization of AgNWs incubated in DCCM-1 for 0.25 h at 37 °C. (a) A BF-TEM image showing the formation of particulates on the AgNW surface. The boxed area was further analyzed by HRTEM (b), the lattice spacing of the particles was 0.218 ± 0.007 nm which is close to the Ag₂S (031)

interplanar spacing. The presence of sulfur was further confirmed by STEM-EDX. A representative EDX spectra collected from the edge of the AgNWs is shown in (c).

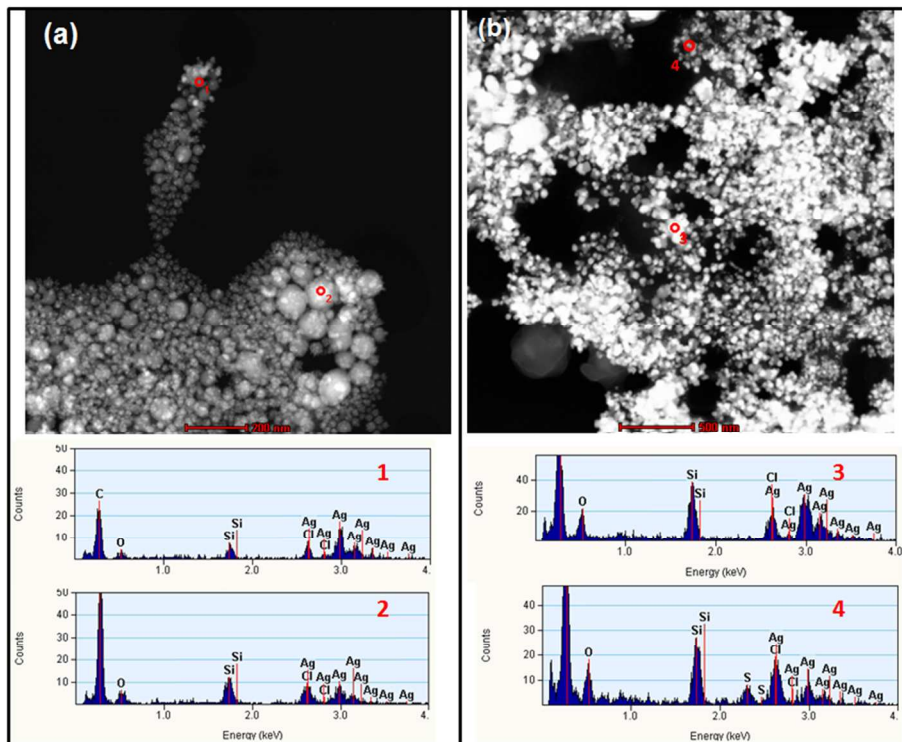


Figure 5S. HAADF-STEM-EDX characterization of precipitates formed after the incubation of 17.0 $\mu\text{g/mL}$ AgNO_3 (equal to an Ag concentration of 10 $\mu\text{g/mL}$) in (a) RPMI-1640 and (b) DCCM-1at 37 $^\circ\text{C}$ for 0.5 h. The corresponding STEM-EDX spectra 1-4 were collected from area 1-4 marked in (a-b). The precipitation were collected by filtering the solution through 2 kDa filter membrane and washed 3 times by DI-water.

HAADF-STEM image (Fig. 5Sa) shows the morphology of the precipitates formed by adding Ag^+ into RPMI-1640. The particles have sizes range from ~ 20 to ~ 200 nm, which can not pass the 2 kDa filter membrane through centrifuge filtering process or will be easily centrifuged down together with unreacted Ag nanomaterials during simple centrifugation separation process. These precipitates likely to be a mixture of silver oxide (the solubility constant $K_{\text{sp}} = 4 \times 10^{-11}$) and silver chloride ($K_{\text{sp}} = 1.77 \times 10^{-10}$) as

indicated by the presence of Ag, O and Cl signals as shown in Fig. 5Sa, spectral1-2. Similar precipitates were also formed in DCCM-1 (Fig. 5Sb). But as compared to RPMI-1640, except formation of silver oxide and silver chloride (Fig. 5Sb, spectrum 3), the insoluble compounds formed in DCCM-1 likely contain silver sulfide (Fig. 5Sb, spectrum4). A potential question is why there is no formation of silver chloride or silver oxide formed in the case of incubation of AgNWs in DCCM-1. This is because Ag^+ ions were directly rapidly into the DCCM-1 in this control experiment. This condition is different to the case of incubation of AgNWs in DCCM-1. In the AgNWs case, the availability of Ag^+ is limited by the extremely slow oxidation dissolution process. On the other hand, the formation of silver sulfide is thermodynamic preferred, as it has a much lower solubility with a $K_{sp} = 5.92 \times 10^{-51}$. Therefore, there will be no formation of silver chloride and silver oxide before the complete consumption of sulfide species. Our recent publication reported similar phenomenon inside lung epithelial cells, only formation of silver sulfide rather than silver chloride and oxide was detected inside cellular environment.⁵

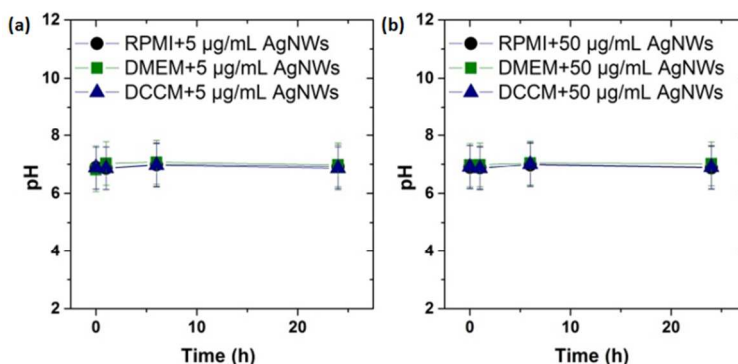


Figure 6S. Time-resolved pH measurements of soluble sulphur concentrations during incubation of AgNWs with PRMI-1640, DMEM and DCCM-1 at 5 and 50 µg/mL (Ag-atom basis) respectively.

Fig 6S shows no significant pH variations were observed for all three cell media for both AgNWs concentrations. First of all, no significant pH changes were expected for DMEM and RPMI-1640, as there is no sulfidation reaction and extremely low oxidation dissolution rate of AgNWs. Second of all, cell media have high buffer capacities, even if there is sulfidation reaction, like the case for DCCM-1 cell media, the consumption of H^+ or generation of OH^- is not enough to change the pH of cell media. For

example, DMEM has a buffer capacity of 11.3 mM/pH,⁶ which means 11.3 mM strong acid or base is needed to change the pH by 1 unit. For 5 and 50 $\mu\text{g/mL}$ AgNWs, which are equivalent to 0.046 mM and 0.46 mM Ag atoms respectively, the consumption of H^+ or generation of OH^- can be estimated to be from 0.046 to 0.46 mM in the extreme case of assuming a 100 % reaction.

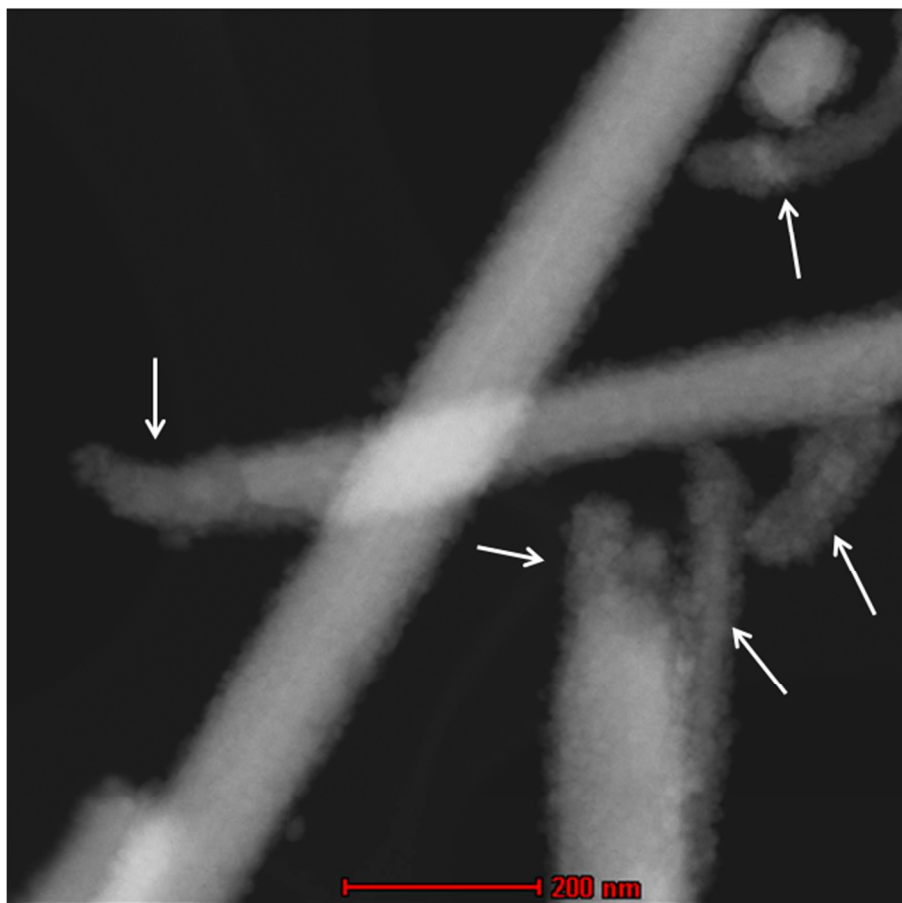


Figure 7S. HAADF-STEM image of AgNWs incubated in DCCM-1 filtrate at 37 C for 6 h. The arrows indicate significantly sulfidized NWs tips or completely sulfidized NWs.

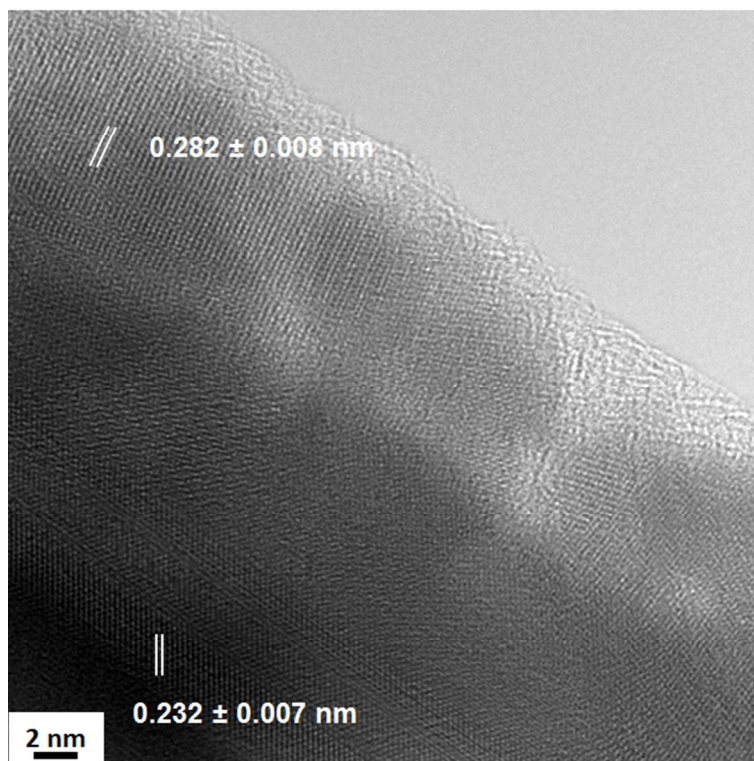


Figure 8S. HRTEM analysis of AgNWs incubated in DCCM-1 filtrate (separated small molecule solutes and salts) at 37 °C for 6 h. The interplanar spacings measured from the surface and core of the nanowires is $0.282 \pm 0.008 \text{ nm}$ and $0.232 \pm 0.007 \text{ nm}$, which are consistent with lattice spacings of Ag_2S (-112) and Ag (111) facets respectively.

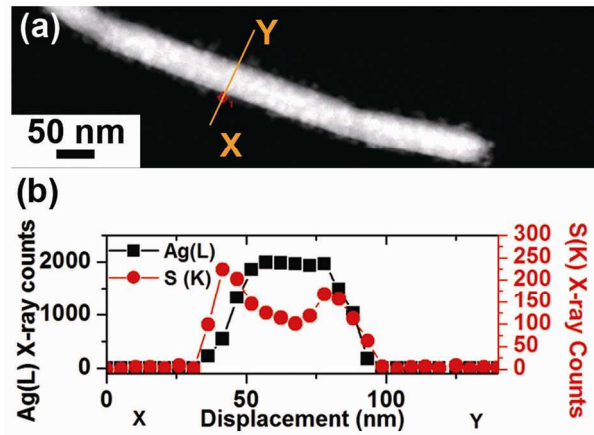


Figure 9S. (a) A HAADF-STEM image of the area illustrated in Fig. 4c. A STEM-EDX line profile was collected along the line XY. (b) The X-ray counts within an energy window around the Ag (L) and S (K) peaks in the EDX spectrum were extracted along the line X-Y and indicate that a silver sulfide layer has formed on the AgNW surface.

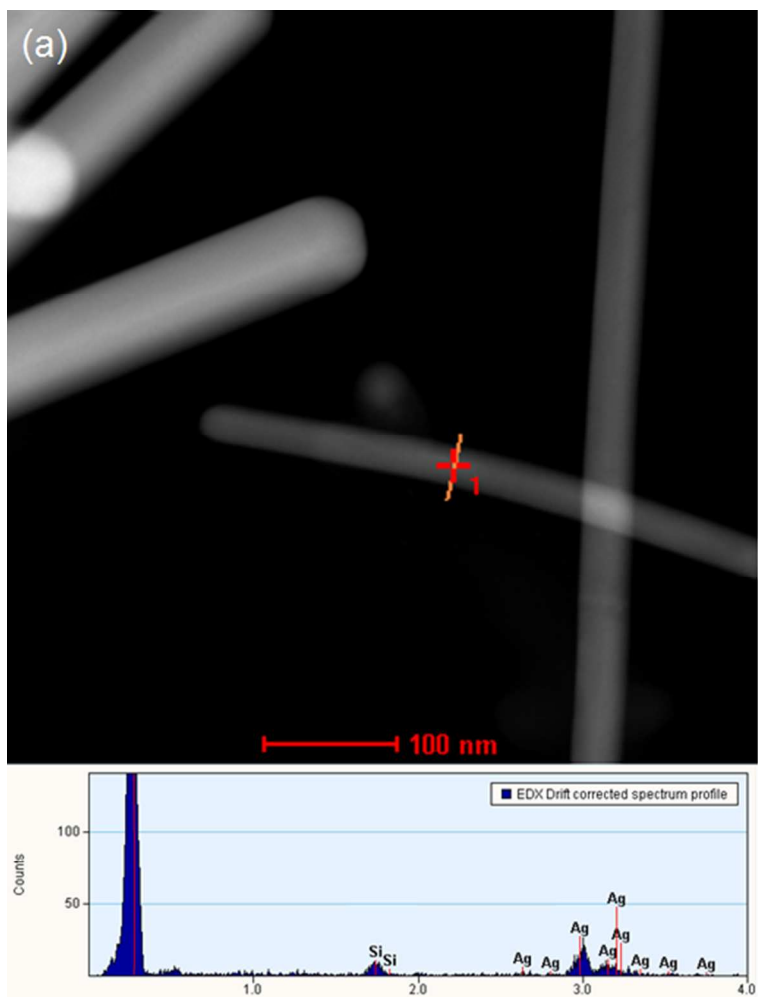


Figure 10S. A HAADF-STEM image of AgNWs incubated with separated proteins from DCCM-1. A STEM-EDX line profile was collected along the line. The EDX spectrum collected from the core of the AgNWs (marked by the cross) is presented.

Table 2S. The formulation of DMEM^{*}, RPMI-1640^{*} and DCCM-1[#]. ^{*} Information was provided by Sigma-Aldrich. [#]The component of DCCM-1 is confidential, relevant information presented here was extracted from literature.³

DMEM (D6546-Sigma)			RPMI-1640 (R7638-Sigma)			DCCM-1 (Bioind)	
Inorganic Salts	Estimated conc. (ppm)	Estimated Sulfur conc. (ppm)	Inorganic Salts	Estimated conc. (ppm)	Estimated Sulfur conc. (ppm)	Inorganic Salts	ppm
Calcium Chloride	200	0	Calcium Nitrate • 4H ₂ O	100	0	confidential	
Ferric Nitrate • 9H ₂ O	0.1	0	Magnesium Sulfate (anhydrous)	48.84	13.0	Amino Acids	
Magnesium Sulfate (anhydrous)	97.67	26.0	Potassium Chloride	400	0	confidential	
Potassium Chloride	400	0	Sodium Bicarbonate	1000	0	Proteins	
Sodium Bicarbonate	3700	0	Sodium Chloride	6400	0	human albumin	not available
Sodium Chloride	6400	0	Sodium Phosphate Dibasic (anhydrous)	800	0	human transferrin	not available
Sodium Phosphate Monobasic (anhydrous)	109	0	Amino Acids			globulins	not available
Amino Acids	0	0	L-Alanyl-L-Glutamine	—			
L-Arginine • HCl	84	0	L-Arginine	200	0		
L-Cystine • HCl	62.6	7.2	L-Asparagine (anhydrous)	50	0		
L-Glutamine	—	—	L-Aspartic Acid	20	0		
Glycine	30	0.0	L-Cystine • 2HCl	65.2	7.5		
L-Histidine • HCl • H ₂ O	42	0.0	L-Glutamic Acid	20	0		
L-Isoleucine	105	0.0	L-Glutamine	—			
L-Leucine	105	0.0	Glycine	10	0		
L-Lysine • HCl	146	0.0	L-Histidine	15	0		
L-Methionine	30	6.4	Hydroxy-L-Proline	20	0		
L-Phenylalanine	66	0	L-Isoleucine	50	0		
L-Serine	42	0	L-Leucine	50	0		
L-Threonine	95	0	L-Lysine • HCl	40	0		
L-Tryptophan	16	0	L-Methionine	15	3.2		
L-Tyrosine • 2Na	103.79	0	L-Phenylalanine	15	0		
L-Valine	94	0	L-Proline	20	0		
Vitamins			L-Serine	30	0		
Choline Chloride	4	0	L-Threonine	20	0		
Folic Acid	4	0	L-Tryptophan	5	0		
myo-Inositol	7.2	0	L-Tyrosine • 2Na • 2H ₂ O	28.83	0		
Niacinamide	4	0	L-Valine	20	0		
D-Pantothenic Acid (hemicalcium)	4	0	Vitamins				
Pyridoxal • HCl	—	0	D-Biotin	0.2	0		
Pyridoxine • HCl	4	0	Choline Chloride	3	0		
Riboflavin	0.4	0	Folic Acid	1	0		
Thiamine • HCl	4	0	myo-Inositol	35	0		
Other	0	0	Niacinamide	1	0		
D-Glucose	4500	0	p-Aminobenzoic Acid	1	0		
HEPES	—	0	D-Pantothenic Acid (hemicalcium)	0.25	0		
Phenol Red • Na	15.9	0	Pyridoxine • HCl	1	0		
Pyruvic Acid • Na Add	110	0	Riboflavin	0.2	0		
Glucose	—	0	Thiamine • HCl	1	0		
L-Glutamine	584	0	Vitamin B12	0.005	0		
Sodium Bicarbonate	—	0	Other				
			D-Glucose	2000	0		
			Glutathione (reduced)	1	0		
			HEPES	4770	640.5		
			Phenol Red • Na Add	5.3	0		
			L-Glutamine	300	0		
			Sodium Bicarbonate	—			

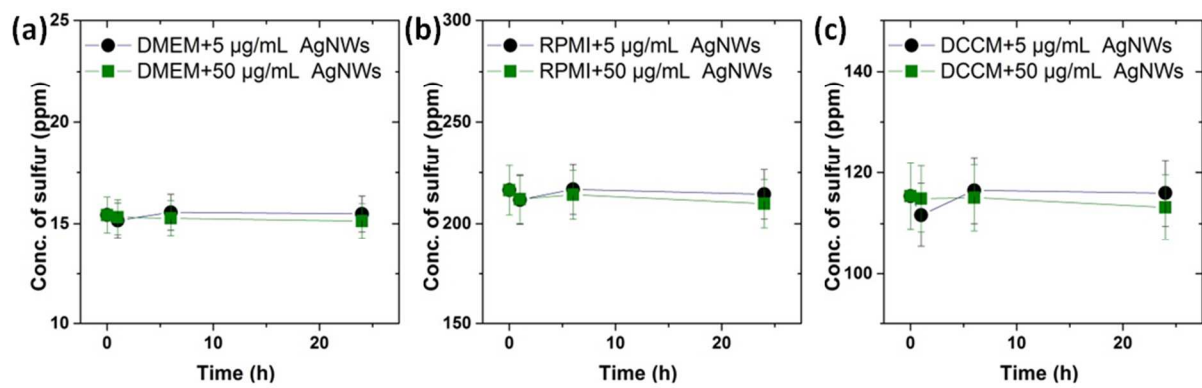


Figure 11S. Time-resolved ICP-OES measurement of soluble sulphur concentrations during incubation of AgNWs with PRMI-1640 (a), DMEM (b) and DCCM-1 filtrates (filtered through 2 kDa membrane) (c) at 5 and 50 $\mu\text{g/mL}$ on Ag-atom basis.

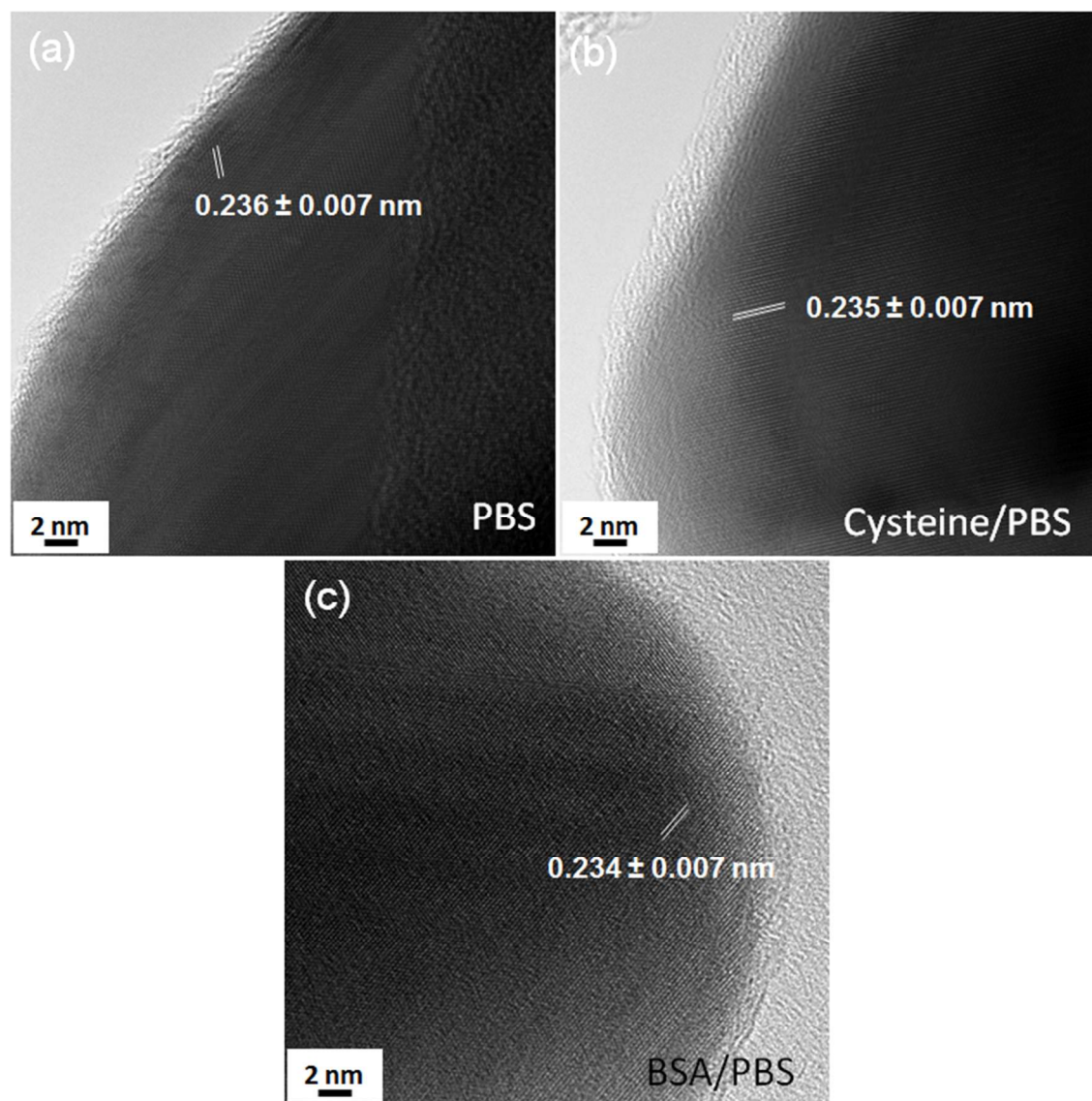


Figure 12S. HRTEM analysis of AgNWs incubated in (a) PBS, (b) PBS+cystine and (c) PBS+BSA at 37 °C for 6 h. HRTEM images show no alternation of AgNWs morphology. The interplanar spacings measured from the nanowires are consistent with lattice spacings of Ag (111) facets.

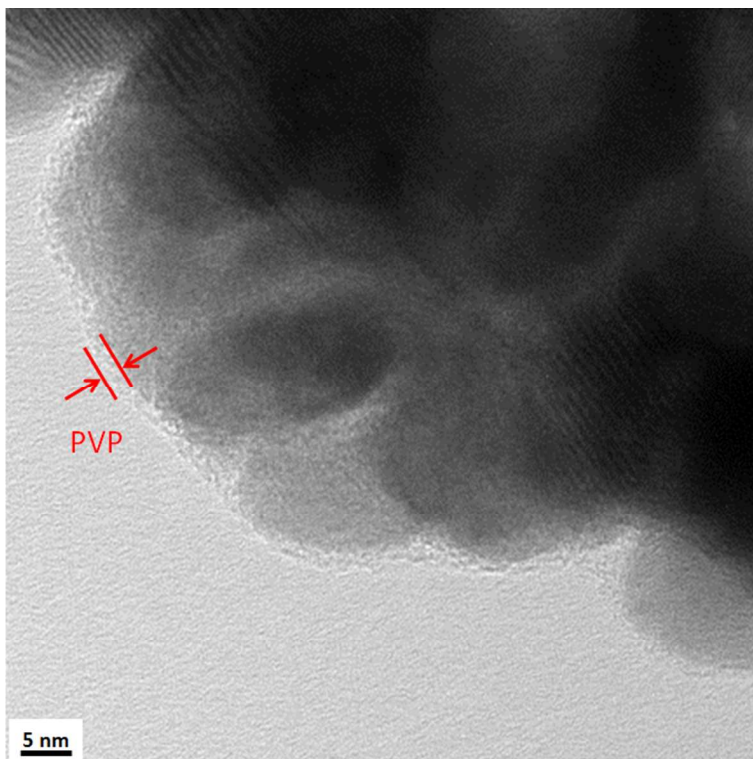


Figure 13S. HRTEM image shows the presence of PVP layer(s) on the sulfidized surface of AgNWs.

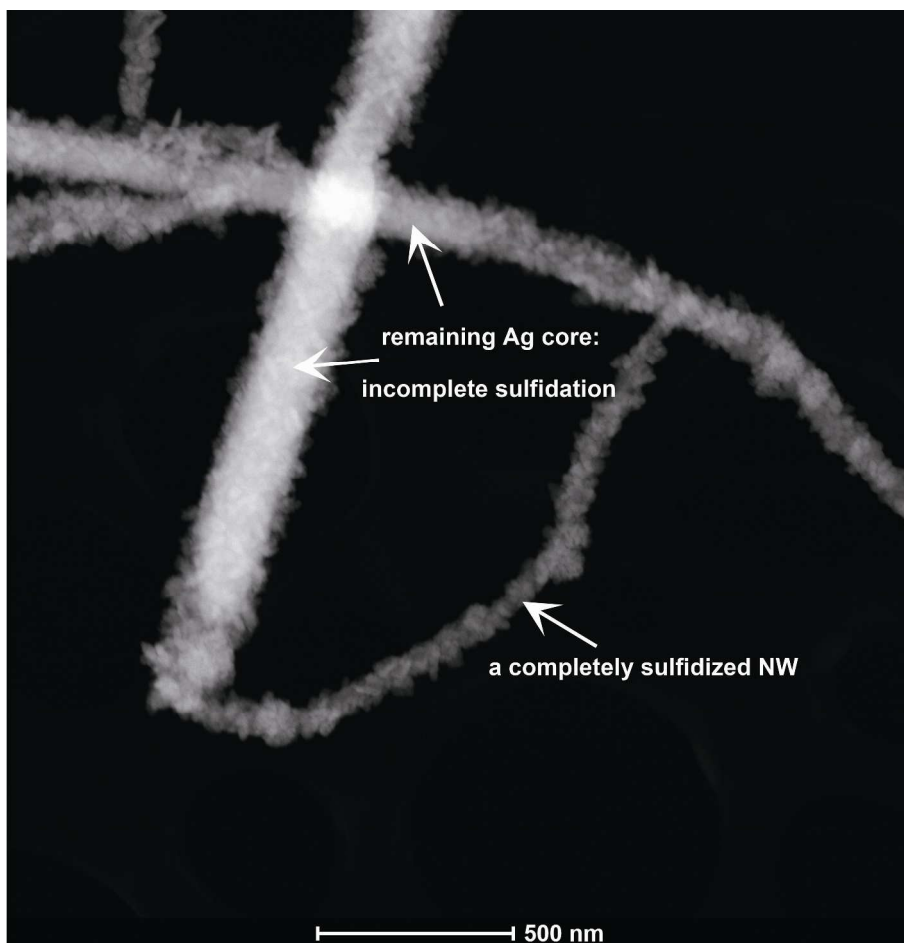


Figure 14S. A HAADF-STEM image of AgNWs incubated in DCCM-1 for 6 h. AgNWs with larger diameters appear to have incompletely sulfidized, indicated by the remaining silver core underneath the sulfidized surface. In contrast, the smaller diameter AgNWs appear to have been completely sulfidized.

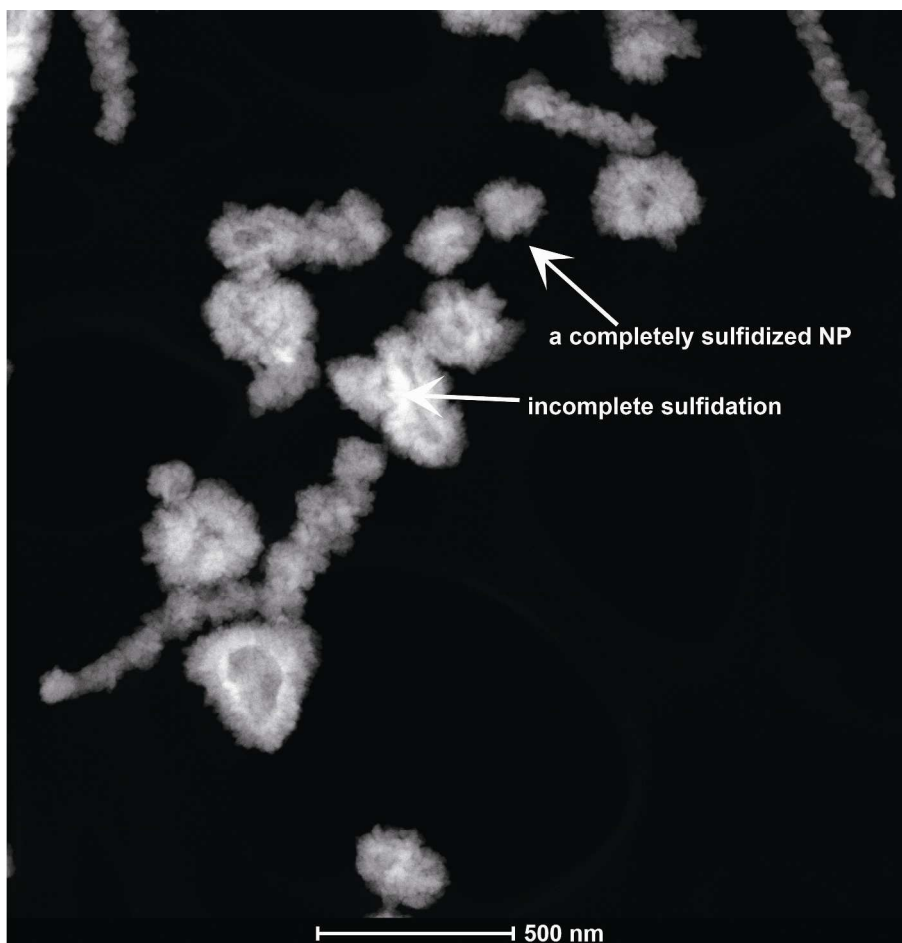


Figure 15S. A HAADF-STEM image from a region displaying a mixed population of AgNWs and AgNPs, incubated in DCCM-1 for 24 h. The AgNPs followed same trend of forming core shell structures as the AgNWs. Depending on size, they show partial or full sulfidation.

Reference

1. Sun, Y.; Xia, Y., Large-Scale Synthesis of Uniform Silver Nanowires Through a Soft, Self-Seeding, Polyol Process. *Advanced Materials* **2002**, *14*, (11), 833-837.
2. <http://rsb.info.nih.gov/ij/>.
3. Ruenraroengsak, P.; Novak, P.; Berhanu, D.; Thorley, A. J.; Valsami-Jones, E.; Gorelik, J.; Korchev, Y. E.; Tetley, T. D., Respiratory epithelial cytotoxicity and membrane damage (holes) caused by amine-modified nanoparticles. *Nanotoxicology* **2012**, *6*, (1), 94-108.
4. *The International Centre for Diffraction Data (ICDD), PDF2 database.*

5. Chen, S.; Goode, A. E.; Sweeney, S.; Theodorou, I. G.; Thorley, A. J.; Ruenraroengsak, P.; Chang, Y.; Gow, A.; Schwander, S.; Skepper, J.; Zhang, J. J.; Shaffer, M. S.; Chung, K. F.; Tetley, T. D.; Ryan, M. P.; Porter, A. E., Sulfidation of silver nanowires inside human alveolar epithelial cells: a potential detoxification mechanism. *Nanoscale* **2013**, *5*, (20), 9839-47.
6. Acker, H.; Carlsson, J.; Holtermann, G.; Nederman, T.; Nylén, T., Influence of glucose and buffer capacity in the culture medium on growth and pH in spheroids of human thyroid carcinoma and human glioma origin. *Cancer Res* **1987**, *47*, (13), 3504-8.